



Benefits of Blue Carbon Stocks in a Coastal Jazan Ecosystem Undergoing Land Use Change

Hazem T. Abd El-Hamid¹ · Ebrahim M. Eid^{2,3} · Mohamed H.E. El-Morsy^{4,5} · Hanan E.M. Osman^{6,7} · Amr E. Keshta⁸

Received: 5 July 2022 / Accepted: 29 August 2022
© The Author(s) 2022

Abstract

Coastal ecosystems are characterized by high content of soil carbon storage; however, they experience severe land conversions in the past decades. The current study aims to examine how different land use/land cover (LU/LC) impact carbon stock in coastal ecosystem along Jazan coast, Saudi Arabia. In this study, impacts of LU/LC on carbon stocks in the coastal zone of Jazan, Saudi Arabia in 2009, 2013, and 2021 were assessed. Also, the LU/LC dynamics were evaluated using data provided by the land use dynamic model. The carbon stocks were modelled based on LU/LC using the InVEST program. Our study results showed that the decrease in mangroves from 2013 to 2021 reflects the high atmospheric emissions of carbon dioxide (CO₂). Also, the increase in built-up areas might negatively impact total carbon stock. The estimated carbon stocks for the coastal zone of Jazan biome were 7279027.42 Mg C in 2009 (1Mg = 10⁶ g). It decreased to 2827817.84 Mg C in 2013, with a total loss of -4450675.40 Mg C, and an average of annual loss of -1,112,669 Mg C in the study period with net value of -461240790.53 US\$. On the other hand, the total estimated carbon stock was increased from 2013 to 2021 with a 3772968.31 Mg C in 2021 (a total gain 944840.87 Mg C). Based on the current findings, we recommend that land-use-policy makers and environmental government agencies should implement conservation policies to reduce land use change at Jazan coastal ecosystems.

Keywords Blue carbon · Coastal wetlands · Global warming · InVEST model · Red Sea · Habitat conservation

✉ Amr E. Keshta
akeshta@umd.edu
Hazem T. Abd El-Hamid
hazem_ecology@yahoo.com

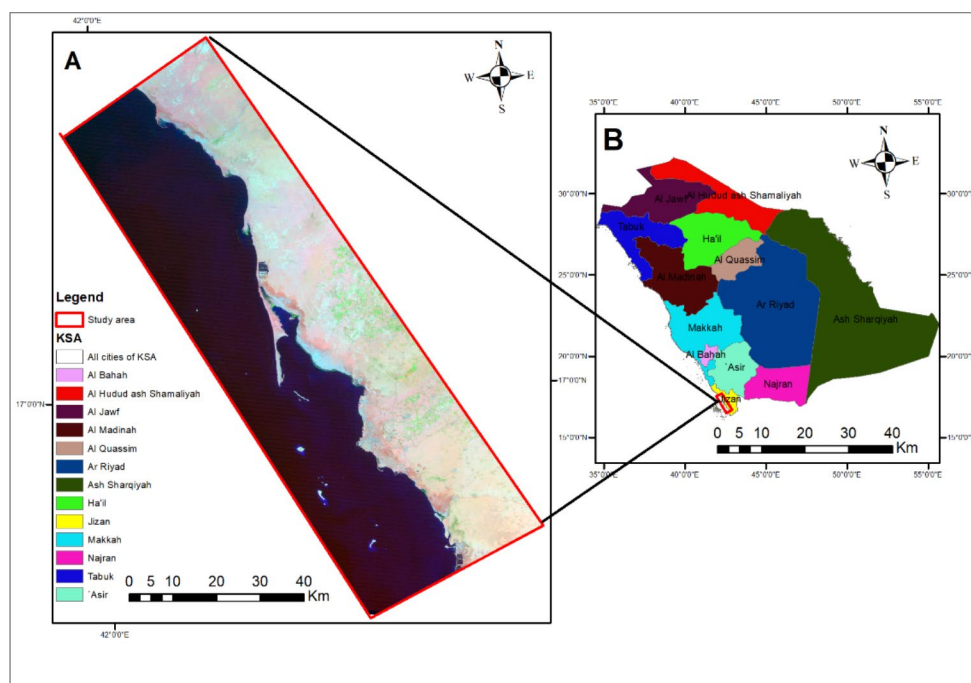
- ¹ National Institute of Oceanography and Fisheries, 11865 Cairo, Egypt
- ² Biology Department, College of Science, King Khalid University, 61321 Abha, Saudi Arabia
- ³ Botany Department, Faculty of Science, Kafrelsheikh University, 33516 Kafr El-Sheikh, Egypt
- ⁴ Deanship of Scientific Research, Umm Al-Qura University, 24243 Makkah, Saudi Arabia
- ⁵ Plant Ecology and Range Management Department, Desert Research Center, 11753 Cairo, Egypt
- ⁶ Biology Department, Faculty of Science, Umm-Al-Qura University, 24243 Makkah, Saudi Arabia
- ⁷ Botany and Microbiology Department, Faculty of Science, Al-Azhar University, 11651 Cairo, Egypt
- ⁸ Botany Department, College of Science, Tanta University, 31512 Tanta, Egypt

Introduction

The continuous increase of greenhouse gases emissions including carbon dioxide (CO₂) is mainly due to fossil fuel combustion and changes in land use practices including those caused by deforestation (IPCC 2007). Emission of CO₂ significantly impacts global warming and climate change as evident in its increased concentration from 280 ppmv in 1850 to 411 ppmv in 2019 (Page 2019). Many scientists have recommended alleviating the impact of climate change through CO₂ sequestration in soil organic carbon (SOC) (Siikamäki et al. 2012a; Taillardat et al. 2018). Moreover, to follow the Paris Climate Agreement's climate recommendations, it is recommended to increase SOC stocks and protect carbon rich soils (e.g., coastal wetlands) from negative impacts including land conversions of natural habitats to agricultural lands (Rumpel et al. 2018; Keshta et al. 2022).

Apart from geologic and oceanic stocks, soil is a fundamental global carbon stock (approximately 1400–1600 Pg; 1Pg = 10¹⁵ g), that can store up to 4.5 times more carbon than

Fig. 1 Location map showing: (A) the study area; and (B) major cities of Saudi Arabia



the earth's total biomass and 3.3 times more carbon than the atmosphere (Post et al. 1982; Eswaran et al. 1993). The carbon that is concealed in coastal ecosystems is called “blue carbon” (Siikamäki et al. 2012b). Coastal wetland soils can store about 450 Pg carbon and form nearly one-third of the global carbon stocks (~1550 Pg) (Bai et al. 2016). Also, coastal wetlands can accumulate carbon as 30–50 times more than forest per unit area (McLeod et al. 2011; Ouyang and Lee 2013), which emphasizes their importance to the global carbon cycle (Howard et al. 2017). Coastal wetlands are among the most productive and biologically diverse ecosystems in the world (Barbier et al. 2011). Moreover, coastal ecosystems have many ecosystem services and functions including carbon storage, flood protection, water treatment, climate regulation, and other services that help local communities to overcome poverty (Costanza et al. 1997).

At regional and global scales, land use change detection using satellite imagery is a fundamental tool for assessing the impacts on soil C stocks. Remote sensing has many applications including assessing land use changes for coastal ecosystems. Mulders 2001, concluded that satellite imagery obtained for the same area at different time intervals is one of the most used methods to estimate the temporal changes in land use. For an efficient and best-productive land use management, Sharma et al. 2019 reached to a conclusion that the assessment of land use changes through satellite imagery interpretation would lead into increasing C stocks and minimizing C emissions. Remote sensing is a powerful tool for assessing global C inventories since the obtained satellite imagery through different sensors (e.g. optical devices and radar, etc.) cover large areas of land and

give higher quality C estimations at lower cost (Richards 2013).

Our current study is a part of a series of articles that aim to assess SOC stocks in various Saudi Arabian coastal wetlands (Eid et al. 2016, 2019, 2020; Arshad et al. 2018; Sanderman et al. 2018; Shaltout et al. 2020). Accordingly, the goal of the current study was to assess land use/land cover impacts on blue carbon storage of coastal ecosystems along Jazan coast, Saudi Arabia. Studying the impacts of land use changes on coastal blue carbon stocks would provide baseline information and guidelines for implementing coastal wetland restoration along Saudi Arabia's Red Sea coast to help policy makers and government agencies to maximize benefits and ecosystem services provided by coastal ecosystems.

Materials and Methods

Study Area

Jazan city is located in the southwest of Saudi Arabia on the border with Yemen and west of the Red Sea (Fig. 1). It is located along the 42° and 43.8° E longitude and between 16.5° and 17° N latitude. It has an area of 13,500 km² with a population of about 1.5 million. According to 2030 country's vision, the coastal zone of Jazan has important projects to support urbanization and industrial activities (Al-Hatim et al. 2015). The terrain of Jazan city varies, while the coastal area extends from north to south. Salt marshes are one of the most common coastal wetland habitats, while Tihama area

is the most fertile area of Jazan. Jazan also has more than 100 islands on the Red Sea. The city can be divided into three parts: inland areas, forests, and plains. The interior area is a series of mountains and forests with rich pastures, plains rich in crops such as coffee beans, grain crops (e.g., barley), and fruits (e.g., grapes). It also contains some types on mangrove in the coastal zone.

Data Collection and LU/LC Dataset

To analyze the LU/LC changes, data were extracted from three cloud-free Thematic Mapper (TM), Enhanced Thematic Mapper (ETM), and Operational Land Imager (OLI) satellite images that obtained in 2009, 2013, and 2021. Landsat images with resolution and low cloud were downloaded using United States Geological Survey (USGS) (<http://glovis.usgs.gov>). All images were referenced using UTM system, zone 36 N and then were radiometry corrected using FLASH atmosphere correction using ENVI 3.5 for further analysis. Calibrations were required to eliminate errors occurred during acquisition procedure (Abd El-Hamid et al. 2019).

Vegetation Index

Vegetation indices were computed using NDVI (Normalized Difference Vegetation Index). NDVI use band 3 (Red) and 4 (Near Infrared) for Landsat 7, and band 4 (Red) with band 5 (Near Infrared) for Landsat 8. NDVI approaching calculation of greenness degree (sea grass, mangroves and agriculture). Vegetation degree of an image correlates with vegetation crown density. NDVI index ranges from -1 to $+1$. Higher NDVI index indicates more crown density. NDVI is formulated as below:

$$\text{NDVI} = \frac{\text{Near} - \text{Red}}{\text{Near} + \text{Red}}$$

Vegetation Cover of Jazan's Coast

Vegetation is the biomass and C storage strength that regulates the climatic change in any area. Presence of vegetation along the study area reflects the C and biomass stock. NDVI is a good indicator of vegetation. NDVI index was classified into six main groups, in our study, as follows (Fig. 2): no vegetation, lowest dense, lower dense, dense, higher dense, highest dense (Zaitunah et al. 2018). In 2009, our results indicated that the class of highest dense was increased from 2009 to 2013 and decreased from 2013 to 2021. Also, some patches of highest dense class were converted to a higher

dense class. The higher dense area represents some forest, planting, and agriculture. Lower and lowest dense were common along coastal and settlement areas (dense populations with human activities). High human accessibilities are also found there, so that land use and land cover are impacting by human activities. The road attracts human for changing land use and land cover. Human will convert forest to agricultural lands, which in turn triggers land use changes. Closer to the roads, forest fragmentation and deforestation increase as a result of the close relationship between building houses and existence of roads. Along Jazan's coast, vegetation landscape is continuously changing as a result of ongoing human activities. Similar to other research findings, our results indicated that the main cause of the C storage loss is related to wetland habitat loss and conversion of natural ecosystems, which are well known by their potential to store C (Lau 2013), due to land built-up (Jiang et al. 2017).

Landsat Classification

The Landsat images were classified into six main classes by using a combination of unsupervised and supervised classification techniques. This is according to skillful information of the LU/LC in the study area and field data of the predominant land cover using Google Earth. The land use and land cover were classified using supervised classification based on the land cover classification system and field observation as ground truth. Every class was identified and drawn using ArcGIS 10.5. (Abd El-Hamid 2020). The field data represent the ground truth. The study area was classified into six classes; open water, vegetation or mangroves, built up, sabkha, and barren. Open water pixels include deep and shallow water, vegetation pixels represent those areas that usually used for growing various plants. Urban pixels represent those areas that include houses, factories, commercial, residential areas, and other places. Finally, bare lands include coastal zone and all desert areas.

LU/LC Prediction Using the CA–Markov Model

For accurate prediction of the LU/LC, Cellular Automata (CA) and the Markov model adopted from IDRISI software were used in the present study (Zhao and Peng 2012). The model used to simulate land use changes and presents the spatial and numerical distribution of transition. Markov model estimates the probability of change from one state to another, taking the LU/LC changes at various times into consideration. In this model, the dynamic change of any

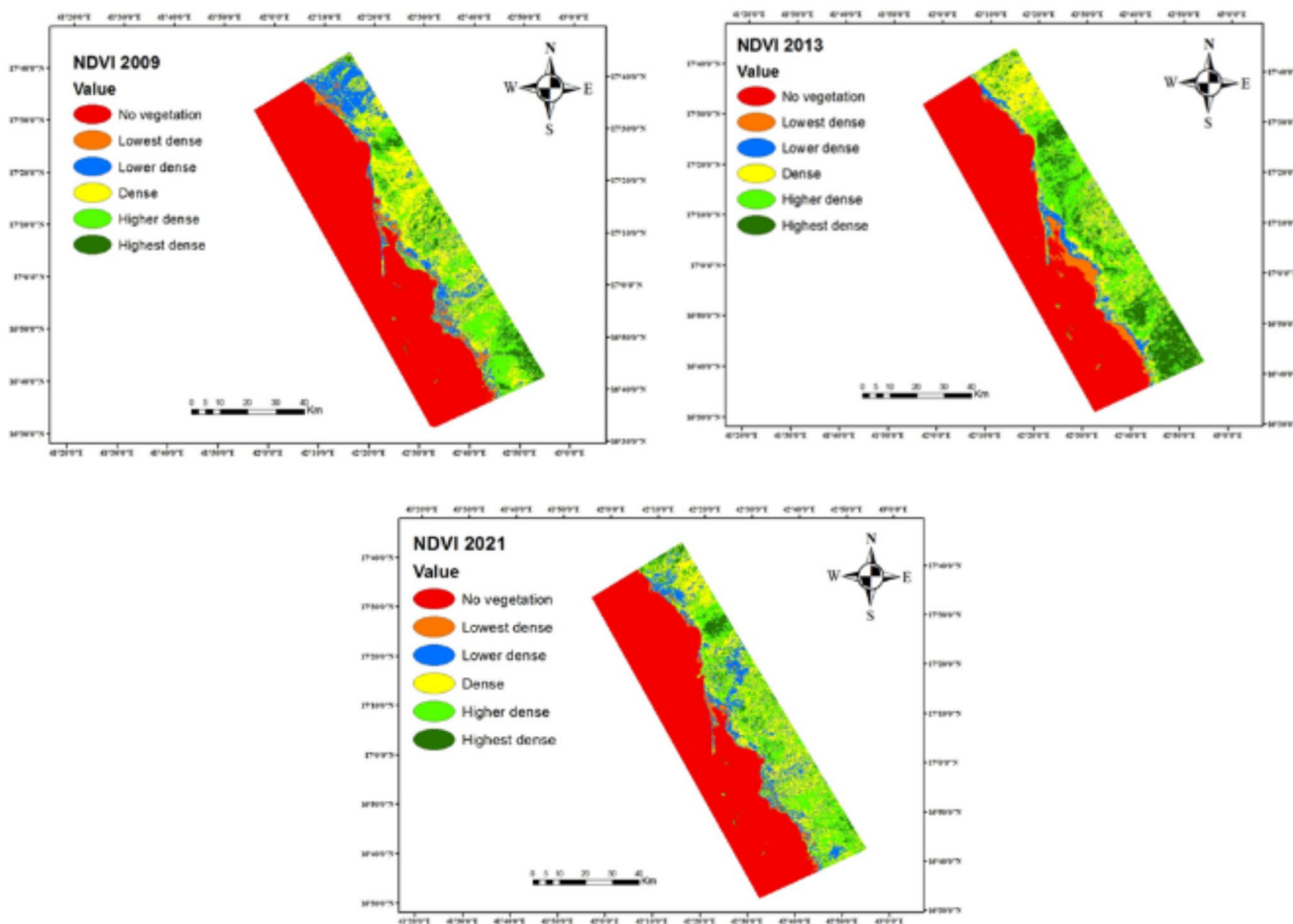


Fig. 2 NDVI classifications during 2009, 2013, and 2021 of Jazan’s coast

study area depends on earlier or current land cover state and calculated using following equations:

$$S_{(t+1)} = (p_{ij} * S_{(t)})$$

$$P_{ij} = \begin{pmatrix} p_{11} & p_{12} & p_{1n} \\ p_{21} & p_{22} & p_{2n} \\ p_{n1} & p_{n2} & p_{nn} \end{pmatrix}$$

$$0 \leq p_{11} \leq 1 \text{ and } \sum_{i=1}^n p_{ij} = 1, i, j = 1, 2, \dots, n$$

Where, $S_{(t)}$ is the state of the system at time t , $S_{(t+1)}$ is the value and state of the system at a time $(t + 1)$; P_{ij} is the transition probability matrix. The reliability of land use change modeling can be improved by joining two or more simulation methods to include the benefits of both. It is well known

that CA–Markov model has been used recently in dynamic spatial phenomenon’s simulation and future land use change prediction.

Validation of simulated LU/LC

The validation of the model is an important part of any prediction-based studies. Kappa index is frequently used for examination the accuracy of the model in many studies. Landis and Koch (1977) stated that if Kappa index is less than or equal to 0.4, it reveals that land use changes greatly with poor consistency between the two images. On the other hand, when Kappa index ranges between 0.40 and 0.75, this indicates obvious changes between the two images with higher consistency. The Kappa index varies from 0 to 1. Values from 0.61 to 0.80 mean substantial, whereas values from 0.81 to 1 mean almost perfect. In this study, Kappa index was 0.81, which indicates that the obtained results are more reliable and with high consistency between the actual observed and predictive results. In this study VALIDATE model was used in IDRISI Selva to compare the predicted

2031 LU/LC with actual 2021 LU/LC to assess the accuracy of the model.

LU/LC dynamic

ESV (Ecosystem Service Value) is mainly affected by natural and man-made factors. ESV has been altered by many factors as construction and other development activities. The land-use intensity not only reflects natural aspects of different land-use types themselves, but also shows the integrative impacts of human factors and natural ecological factors. In the present study, the land-use comprehensive index (L) was introduced to reflect the human activities. It was calculated as following:

$$L = 100 \times \sum_{i=1}^n A_i C_i$$

$$\Delta L_{b-a} = L_b - L_a = 100 \times \left[\sum_{i=1}^n (A \times C_{ib}) - \sum_{i=1}^n (A \times C_{ia}) \right]$$

$$R = \frac{\Delta L_{b-a}}{\sum_{i=1}^n (A \times C_{ia})} = 100 \times \frac{\sum_{i=1}^n (A \times C_{ib}) - \sum_{i=1}^n (A \times C_{ia})}{\sum_{i=1}^n (A \times C_{ia})}$$

From three equations, L denotes the comprehensive index of land use degree, L : 100–400, the closer the L is to 400, the higher the degree of development and utilization; A_i represents the classification index of the land use type; C_i represents the percentage of land use type area; ΔL_{b-a} characterizes the change in the comprehensive index of land use change; L_a and L_b represent the comprehensive land use degree index of a and b time phases; $C_{i.a}$ and $C_{i.b}$ represent the area percentage of the i -type land type in the two stages a and b ; and R characterizes the change rate in land use. To ensure the dynamic of LU/LC in the present study, R has been categorized into three classes as following: (1) if R value more than zero, then the study undergoes development phase; (2) if R value less than zero, then the study undergoes decay phase; and (3) finally if R value equal to zero, then the study undergoes stabilization or adjustment phase.

Carbon quantification

To estimate the amount of carbon (C) storage and sequestration, a new module has been used based on C cycle in the selected study area (He et al. 2016; Tallis et al. 2013). In the current study, there were four C pools that includes aboveground C density, belowground C density, soil organic C, and dead organic matter (Tallis et al. 2013). The calculation of the C storage $C_{m,i,j}$ in a given grid cell (i, j) with land-use type “ m ” can be achieved by the following equation (Aalde et al. 2006):

$$C_{m,i,j} = A \times (C_{am,i,j} + C_{bm,i,j} + C_{sm,i,j} + C_{dm,i,j})$$

In this formula, A is the real area of each grid cell (ha). Also, $C_{am,i,j}$, $C_{bm,i,j}$, $C_{sm,i,j}$, and $C_{dm,i,j}$ are the aboveground C density, belowground C density, soil organic C density, and dead organic matter C density (i, j), respectively. Finally, C storage and sequestration “ S ” can be computed by next equations for the present study area (Aalde et al. 2006):

$$C = \sum_{m=1}^n C_{m,i,j}$$

$$S = C^{T2} - C^{T1}$$

C^{T2} and C^{T1} demonstrate static C storage in years $T2$ and $T1$ ($T2 > T1$). Using InVEST software; LU/LC and biophysical data are used as inputs to calculate the total amount of C stocks (Sharp et al. 2020).

Carbon sequestration valuation

Carbon storage was estimated using the Carbon Sequestration Storage Model (CSSM) using the InVEST program, established by the Natural Capital Project of the University of Stanford, which consists of a compilation of theoretical models that allow the assessment of several ecosystem services (Sharp et al. 2018). Coastal C stocks are dependent on many factors including aboveground biomass (aerial vegetation), dead biomass (dead branches and litter fall), underground biomass (roots), and soil organic matter (SOM). The CSSM model considers C quantity stored in those pools, based on LU/LC maps. The information to estimate the C stocks were based on the LU/LC and C reservoir maps using the CSSM. The CSSM was applied for the study area and for the LU/LC classes considered in the study (Sabkha, mangroves, vegetation and water bodies) for 2009, 2013, and 2021. Changes in C stocks were assessed based on mean values reported in the literature (Villela et al. 2012). The C stocks were estimated for each LU/LC class,

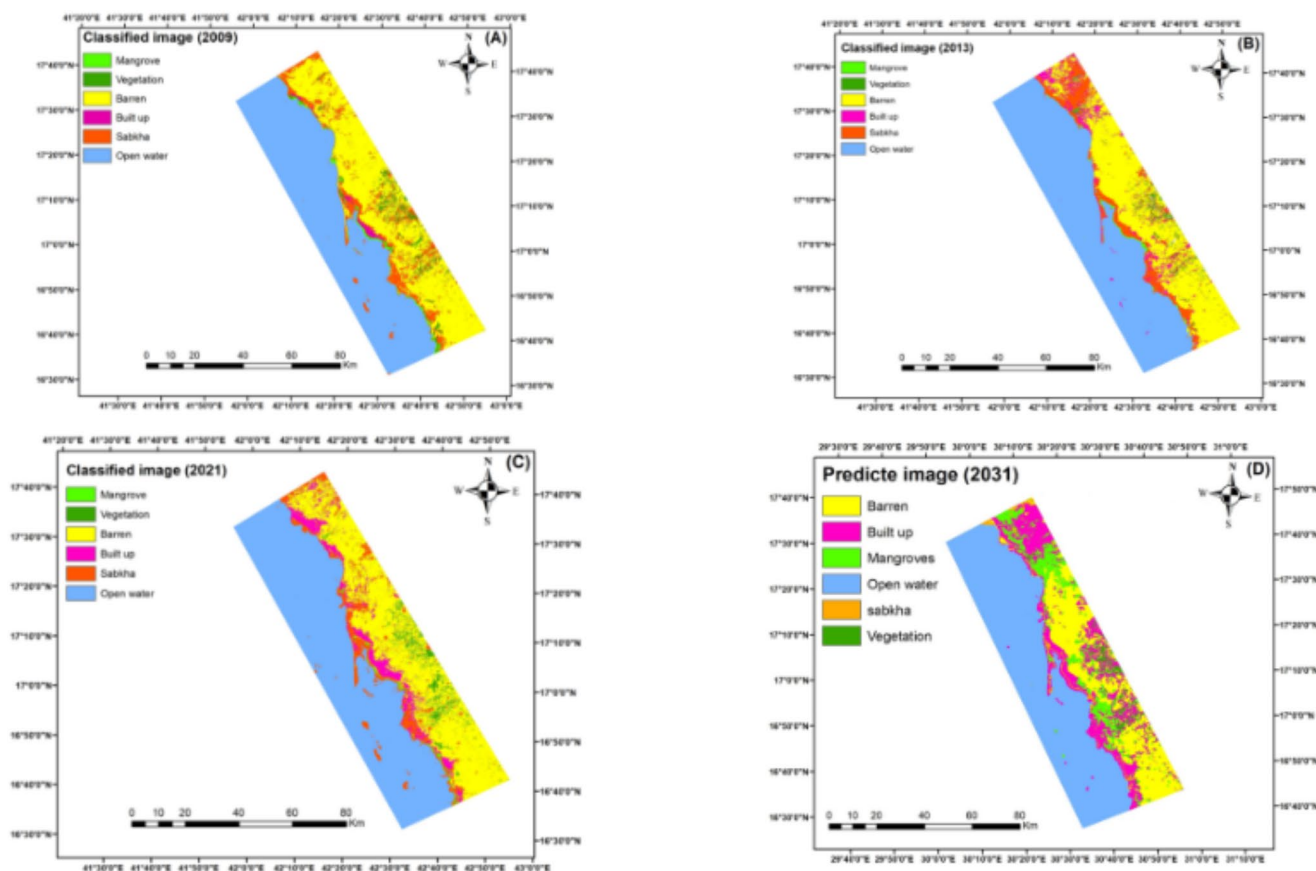


Fig. 3 Land covers maps produced by Landsat image classification: (A) 2009, (B) 2013, (C) 2021; and (D) 2031

and for the four C sets considered in these analyses: above-ground biomass (vegetation), dead biomass (dead branches and litter fall), underground biomass (roots), and SOM. The economic value (expressed as United States Dollar \$) of C stocks was based on estimated values for each year. The estimates indicate values between \$14 and \$41, with a mean of \$24 per Mg CO₂. Carbon social cost provides an estimate linked to socio-environmental costs of climate changes, therefore, more consistent with the reality. Carbon credits denote only the payment of agents, and they did not include the socio-environmental costs of climate changes to the society. This function in the next equation, requires three inputs, including (I) “V,” the monetary value of each unit of carbon, (II) “r,” a monetary discount rate, and (III) “c,” the change in the value of carbon sequestration over time (Tallis et al. 2013):

$$\text{Value}_{\text{seq}_x} = V \frac{\text{sequest}_x}{\text{yr}_{\text{fut}} - \text{yr}_{\text{cur}}} \sum_{t=0}^{\text{yr}_{\text{fut}} - \text{yr}_{\text{cur}} - 1} \left(1 + \frac{r}{100}\right)^{-t} \left(1 + \frac{c}{100}\right)^{-t}$$

The first input “V” is estimated based on the social cost of carbon (SCC) that is released Mg of carbon in the atmosphere in case of excess of the threshold.

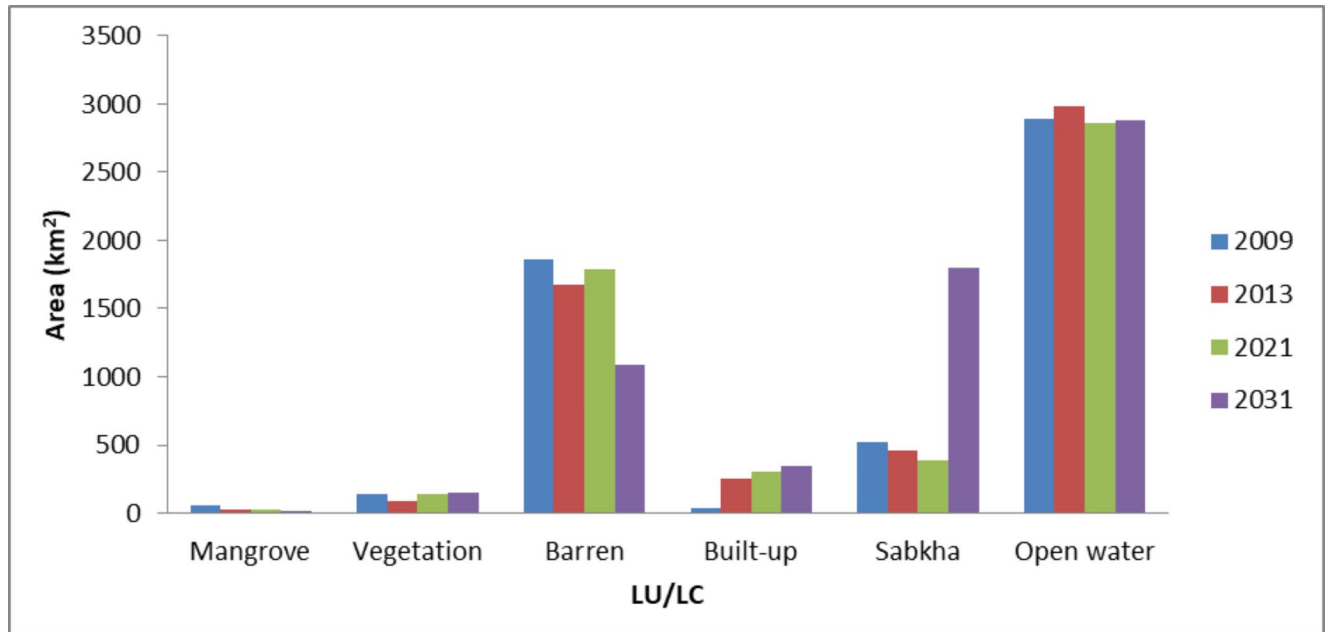
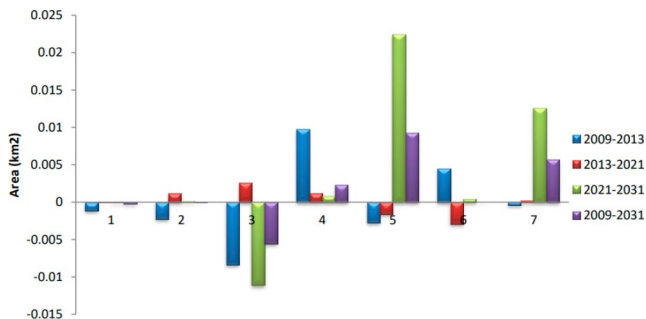
Results and Discussion

Changes in LU/LC during 2009, 2013, 2021, and prediction in 2031

Six classes were extracted; open water, vegetation or mangroves, built up, sabkha, and barren as shown in Fig. 3. The distribution of total area covered by the different LU/LC classes and their percentage of cover in the years of 2009, 2013, 2021, and modeled 2031 are presented in Table 1. Mangroves areas continued their decreasing trend from 2009, 2013, 2021, and modeled 2031, where it decreased from 53.29 km² (0.97%), 28.40 km² (0.52%), 25.79 km² (0.47%) and 20.35 km² (0.39%), respectively. On the other hand, vegetation in the study area reduced from 143.04 km² (2.60%) in 2009 to 93.07 km² (1.69%) in 2013, followed by a rise in 2021 to 143.75 km² (2.61%) and then to 150.26 km² (2.90%) in modeled 2031. Also, barren reduced from 1864.40 km² (33.86%) in 2009 to 1678.85 km² (30.55%) in 2013, followed by a rise in 2021 to 1792.03 km² (32.55%) and then reduced to 1090.71 km² (21.05%) in modeled 2031. On the other hand, built-up areas experienced an increase from 36.38 km² in 2009 to 249.45 km² in 2013, followed by a rise

Table 1 Area (km²) and percentage (%) of LU/LC along the study area periods

LU/LC	2009		2013		2021		2031	
	Area (km ²)	%	Area (km ²)	%	Area (km ²)	%	Area (km ²)	%
Mangroves	53.29	0.97	28.40	0.52	25.79	0.47	20.35	0.39
Vegetation	143.04	2.60	93.07	1.69	143.75	2.61	150.26	2.90
Barren	1864.40	33.86	1678.85	30.55	1792.03	32.55	1090.71	21.05
Built-up	36.38	0.66	249.45	4.54	299.93	5.45	350.01	6.75
Sabkha	521.38	9.47	460.39	8.38	388.51	7.06	1800.24	5.60
Open water	2886.79	52.43	2985.81	54.33	2855.23	51.86	2880.69	63.31

**Fig. 4** Area (km²) of LU/LC during 2009, 2013, 2021 and 2031 of Jazan coast**Fig. 5** Annual rate change of LU/LC (km²) from one year to another

in 2021 to 299.93 km² and then to 350.01 km² in modeled 2031. Sabkha areas continued their decreasing trend from 2009, 2013, 2021 and increased in modeled 2031. Finally, open water in our study area increased from 2886.79 km² (52.43%) in 2009 to 2985.81 km² (54.33%) in 2013, followed by a decrease in 2021 to 2855.23 km² (51.86%) and then increased to 2880.69 km² (63.31%) in modeled 2031 as shown in Fig. 4. Mangroves might have decreased as a result of anthropogenic effects and climatic change. The

increase in built-up area was related to Kingdom of Saudi Arabia's Vision 2030. The annual rate of LU/LC change was shown in Fig. 5. For more details, gain and loss was detected showing the loss amount of barren and the increase amount of vegetation during the period from 2009 to 2013, on the other hand, from 2013 to 2021 mangrove lose large amount of its area. The main factors related to the increasing development land uses at the expense of deteriorating the mangroves and vegetation covers can be attributed to urban expansion (Abbas et al. 2021). Generally, the recent development can mainly change the natural environment during the last periods (Seto and Kaufmann 2003).

CA-Markov Model Validation

Generally, it is important to evaluate the results classified images from classification with real map of the study area. In the current study, the predicted image (2031) was extracted after high accuracy of CA-Markov model. Accuracy of results shows that decreasing and increasing in spatiotemporal rate of each class trustworthy. Therefore,

Table 2 Land use dynamic of LU/LC in the study area periods

LU/LC	2009	2013	2021
Barren	67.73143733	61.09383392	65.10263316
Built-up	3.304501874	22.69440932	27.24072867
Open water	52.43633435	54.32701925	51.86362145
Vegetation	10.39331014	6.773669289	10.44473122
Mangroves	2.904350602	1.550329662	1.40580378
Sabkha	4.735301106	4.188494025	3.528566086
	2009–2013	2013–2021	2009–2021
<i>L</i>	141.5052354	150.6277555	159.5860844
	2001–2011	2011–2021	254.0695356
ΔL	9.122520071	8.958328895	18.08084897
<i>R</i>	0.064467721	0.059473295	0.113298406

L: land-use comprehensive index; ΔL : characterizes the change in the comprehensive index of land use change; *R*: characterizes the change rate in land use

CA-Markov is a trustable model to predict the future LU/LC. CA-Markov is a forecasting model based on historical data collection. Therefore, it analyzes the combination of past tendencies and then it provides future scenarios. However, CA-Markov does not involve any environment and socioeconomic aspects. Moreover, this model considers/analyzes the changes in the selected area and if there are some influential cells it cannot measure them (Von Neumann 1951). In the current study, two validation models were implemented for 2009 to 2013 and for 2013 to 2021. The Kappa statistics such as $K_{standard}$ (0.75), K_{no} (0.84), and $K_{location}$ (0.89) were for the period from 2013 to 2021, while the overall agreement of 0.82 indicates the reasonable performance (78%) of the model. The accuracy assessment of the classified image is acceptable and reasonable for applications. According to the Kappa index of agreement values that exceed the minimum acceptable standard, and they were greater than 80%, our results indicate that there was

agreement between predicted and actual LU/LC map similar to others (Mishra et al. 2014).

Land Use Dynamic and Transition Probabilities

Results of land use dynamic reflect the recent development along the coastal zone of Jazan city. In the current study, the comprehensive index was increased from 2009, 2013, and 2021(141.5, 150.6, and 159.5, respectively, Table 2. All data were in the range of 100–400, representing that land use has been in a reasonable development stage. The comprehensive land use index continued to increase showing high development from the initial year to the final year. The degree of transformation in land use is more than zero. *R* values were 0.0644, 0.0594 and, 0.1132 for 2009, 2013, and 2021, respectively. In general, urbanization is mainly responsible for transformations of agricultural land. The changes in the LU/LC were observed between two periods, from 2009 to 2013 and 2013–2021. About 1528.00, 23.71, 18.98, 2845.00, 174.52, and 54.55 km² of barren, built-up, mangroves, open water, sabkha and, vegetation, respectively, were noted as shown in Table 3. Due to this conversion, mangroves and vegetation lands experienced high expansion, accompanied by significant changes in barren lands. Large area of sabkha and barren were converted into urban area. Table 4 displays the summary of the probability matrix for major LU/LC conversions for all classes in Jazan that took place between 2013 and 2021 of the first scenario. For instance, the probability of change for mangroves to mangroves is very low but the conversion from open water to mangroves is very low but the conversion from open water to open water and from built-up to built-up are very high, 99% and 84%, respectively. Gain and loss of LU/LC were showed in Fig. 6. All cubic trends of LU/LC were observed in Figs. 7 and 8. All cubic trends from one class to another

Table 3 Transition matrix of LU/LC (km²) from 2009 to 2013

LULC	Barren	Built-up	Mangroves	Open water	Sabkha	Vegetation	2013
Barren	1528	2.409	0.40378	0.008	200.37	60.44343	1791
Built-up	161.9	23.71	3.13749	2.785	106.54	1.794579	299
Mangroves	0.020	0.001	18.9840	0.158	1.2327	5.394716	25.7
Open water	-	-	1.1988911	2845	8.7363	-	2855
Sabkha	115	10.21	29.2989	38.53	174.52	20.826278	388
Vegetation	58.98	0.043	0.27045	0.0018	29.818	54.55160	143
2009	1864	36.38	53.2937	2886.7	521.23	143.0106	5504

Table 4 Transition probability (%) of LU/LC from 2009 to 2021

LULC	Mangroves	Vegetation	Barren	Built-up	Sabkha	Open water
Mangroves	0.0456	0.3688	0.2128	0.2220	0.0566	0.0942
Vegetation	0.0724	0.0146	0.8138	0.0986	0.0002	0.0004
Barren	0.2030	0.0436	0.2488	0.4042	0.0139	0.0859
Built up	0.0308	0.0000	0.0004	0.8476	0.0876	0.0334
Sabkha	0.0277	0.0000	0.0118	0.0526	0.1704	0.7375
Open water	0.0000	0.0000	0.0000	0.0000	0.0002	0.9998

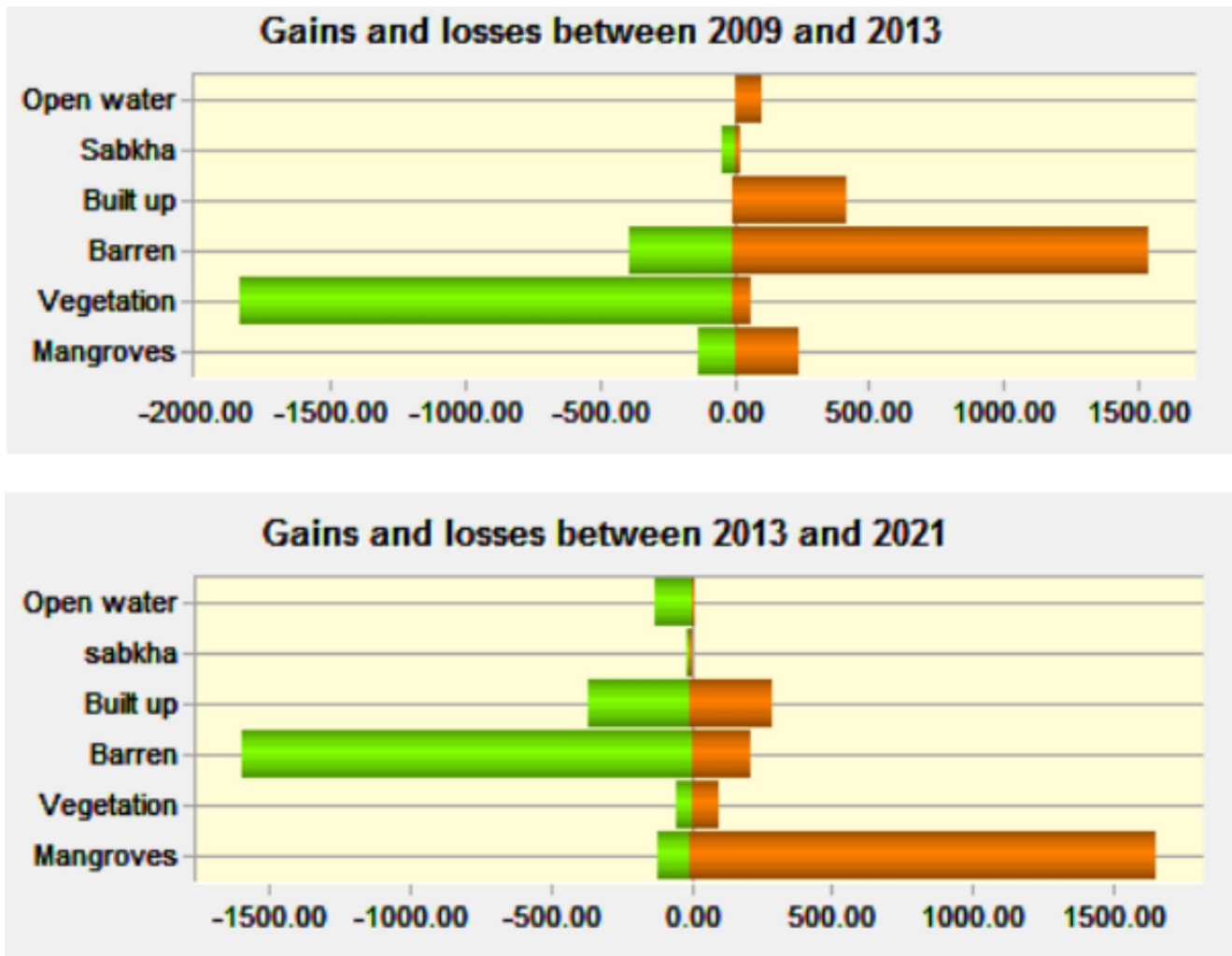


Fig. 6 Gain and loss of LU/LC in Jazan coast

simulate the current situation of the development plan in Jazan city. Also, the transition to mangroves does not appear along the study periods, where the transition to the built-up area appeared in regular manner around the study area.

Carbon Stocks and Sequestration

Our results of C stock for LU/LC classes in the different biomes were modeled using the InVEST program. The spatial distribution of C stock variation in the coastal zone of Jazan is presented in Fig. 9. The estimated C stocks for the coastal zone of Jazan biome was 7279027.42 Mg in 2009. It decreased to 2827817.84 Mg C in 2013, a total loss of -4450675.40 Mg C, an average of annual loss of -1,112,669 Mg C in the study period with net present value of -461240790.53 US\$ as shown in Table 5. On the other hand, the total estimated C stock was increased from 2013 to 2021 with 3772968.31 Mg C in 2021, a total gain of 944840.87 Mg C. Also, the highest stock of C appears

in vegetation area far from water. Also, the C stock spatial distribution for aboveground and belowground is presented in Fig. 10. The expansion of cultivated land and urban areas had a slight influence on C storage, as this change in LU/LC has mainly affected wet lawns and the edges of unused land (Kacem et al. 2022). Mekuria (2013) in his study reported that dense forest had higher total C stock followed by open forest, grassland, cultivated land, and bare land. Our results showed that mangroves and sea grasses have large contribution for the total value of the ecosystem as they provide higher amount of C storage and sequestration. Our study reveals that there is no C in open water area, where the positive change in C is very low that appears in vegetation and mangroves areas. Thus, our results recommend conserving the vegetated areas for sustaining C stock.

According Abd El-Hamid and Hafiz 2022, human disturbances are causing an ongoing decline in total carbon sequestered, which will eventually harm ecosystem services and have an impact on human health.

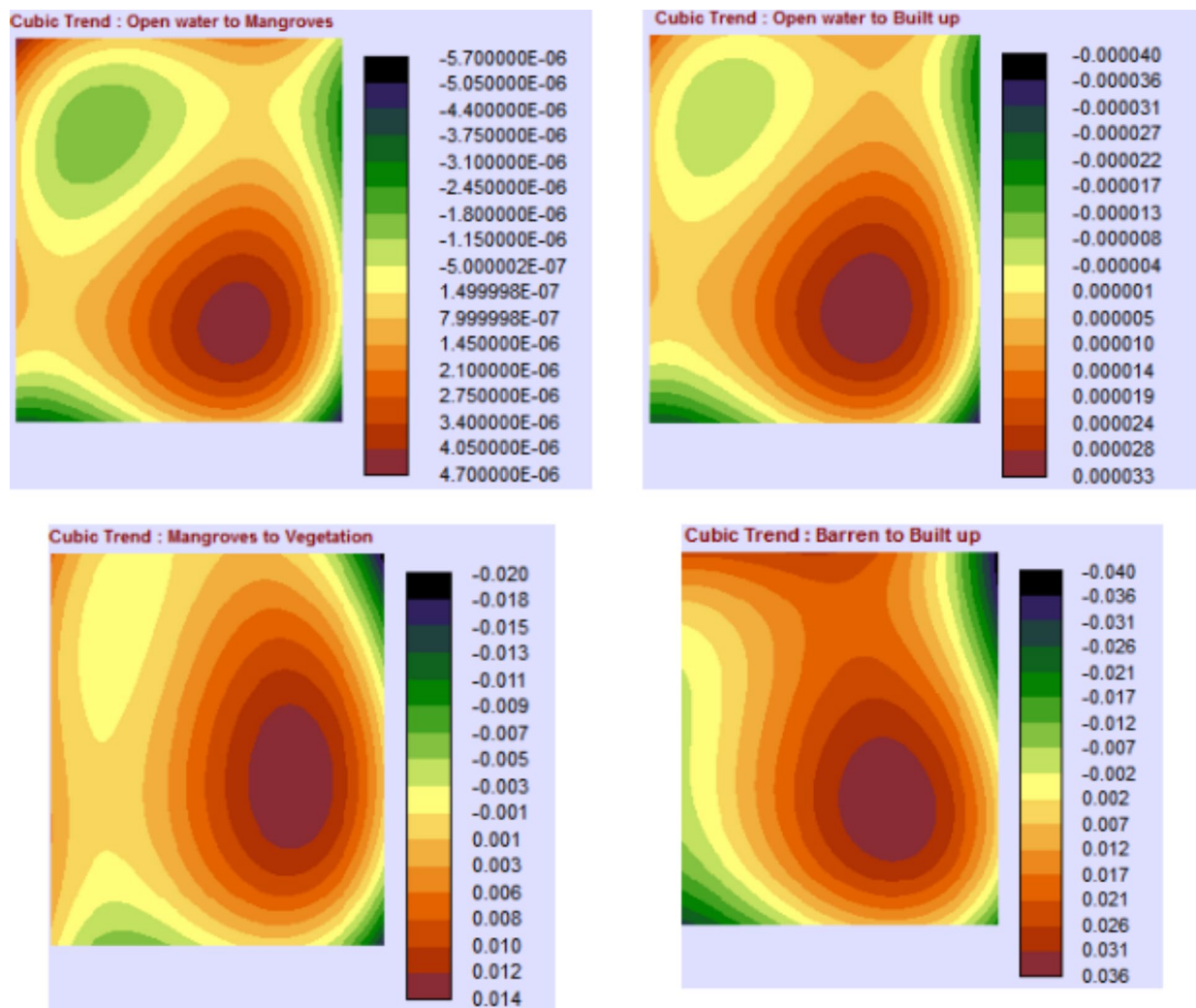


Fig. 7 Cubic trend of LU/LC from 2009 to 2013

The total cost of C stock decreased from 2009 to 2013 and increased from 2013 to 2021. Also, the transition cost of C using three different discount modeling agrees with change in LU/LC as shown Table 6. Our findings are similar to those of Sil et al. (2017), who reported that the value of C sequestration with a different C price flocculated from a minimum of US\$ $13.5 \text{ ha}^{-1} \text{ yr}^{-1}$ when converting forest to grassland. Padilla et al. (2010) reported that the intense anthropogenic activities (conversion of forest to human settlement and farmland) would result in a spatial distribution of C sequestration value that varied from a minimum of US\$ $-1361.23 \text{ ha}^{-1} \text{ yr}^{-1}$ to a maximum of US\$ $230.43 \text{ ha}^{-1} \text{ yr}^{-1}$. Our results indicated that even with the limited data available for simulated and current C storage, it could be an acceptable demonstration of C storage in the study area. Finally, Japelaghi et al. 2022 reported that human activities and its consequences which will lead to severe deforestation and at last the reduction of ecosystem services especially storage and the sequestration of carbon.

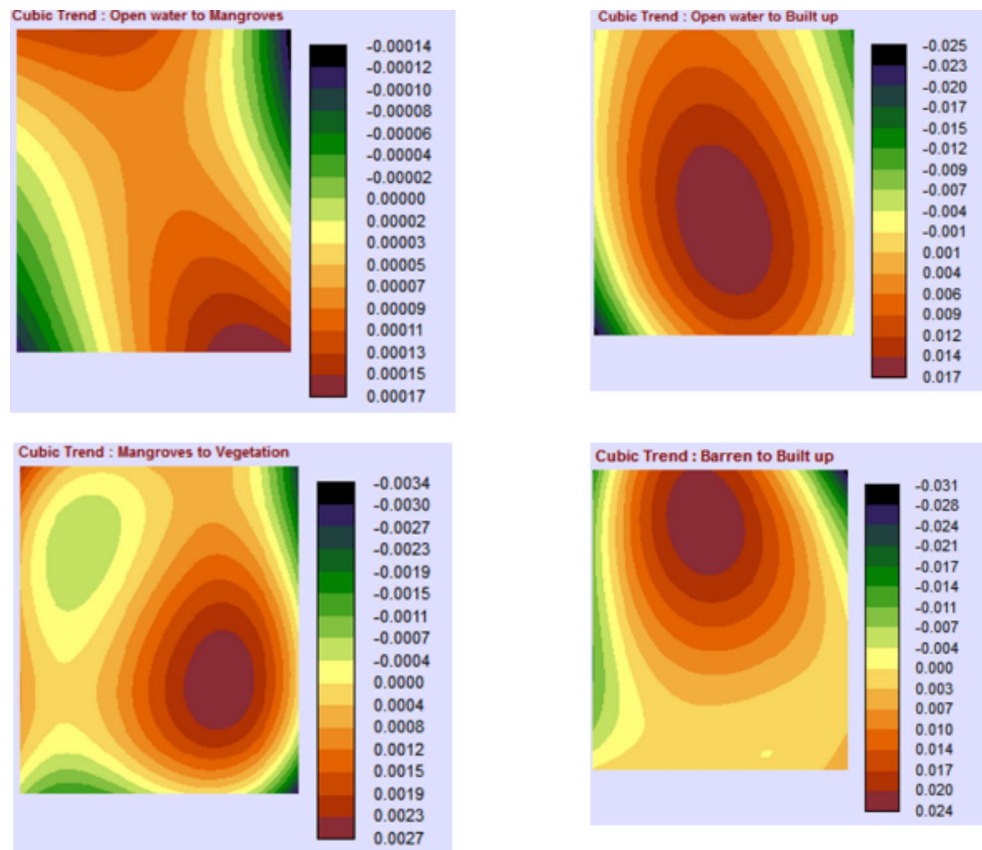
Study limitations

One of the limitations of our study was the lack of detailed and reliable data on C density in various pools of the studied sites. It is known that the deficiency of accurate data about coastal ecosystem might lead into insufficient results about C stocks in different habitats. Also, the LU/LC change might impact the total estimation of C in the current and upcoming periods.

Conclusion

Studying changes in LU/LC provides vital data for policy decision-making in regard to the future of coastal ecosystem services. Our results indicated that the mangrove habitats were significantly decreased since 2013. Moreover, estimated soil C stocks of Jazan were substantially

Fig. 8 Cubic trend of LU/LC from 2013 to 2021



decreased since 2013 (2827817.84 Mg C), with a total loss of -4450675.40 Mg C and an average of annual loss of $-1,112,669$ Mg C during the study time frame (2013–2021) concluding a net value loss of $-461,240,790.53$ US\$. Degradation of the ecosystem along the study area might have negative impacts on blue C storage. So, ecosystem conservation should be taken into consideration for reducing C stock loss. Our results showed that the insufficiency of SOC is likely to increase ecosystem C loss due to change in mangroves and sea grasses along the coastal zone of Jazan city. Therefore, our study investigated the current situation of the mangroves and grasses scattered along the coastline, which might provide an opportunity for officials to take the necessary measures to preserve biological diversity to reduce C emissions in the atmosphere and preserve soil C stocks at coastal wetlands.

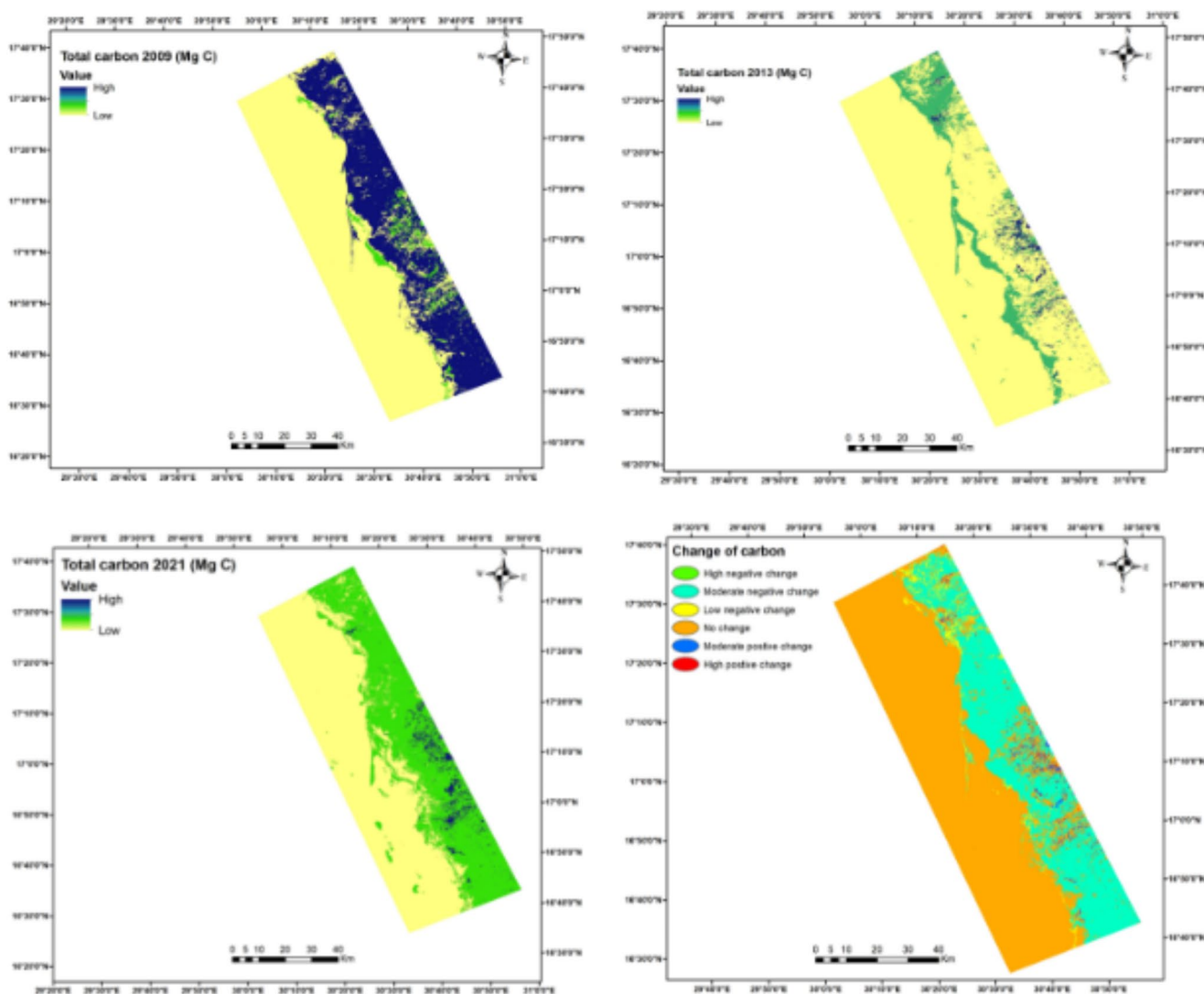


Fig. 9 Spatial distribution and change carbon in the study area

Table 5 Total cost (\$US/km²) of carbon stocks for each LU/LC during study periods

LU/LC	2009	2013	2021	2031
Open water	5861.9	3124.22	2836.9	2238.5
Mixed water	15,734	10,238	15,813	16,529
Floating plants	205,084	184,674	197,123	119,978
Built-up	4002	27,440	32,992	38,501
Barren	57,352	50,643	42,736	198,026
Agriculture	317,547	328,439	314,075	316,876
Carbon storage (Mg C)	7279027.42	2827817.84	3772968.31	-
Total cost/km ²	605580.8	604556.9	605576.4	692148.6
Total cost for year	177,539,697,646	177,239,524,084	177,538,407,687	202,919,004,648

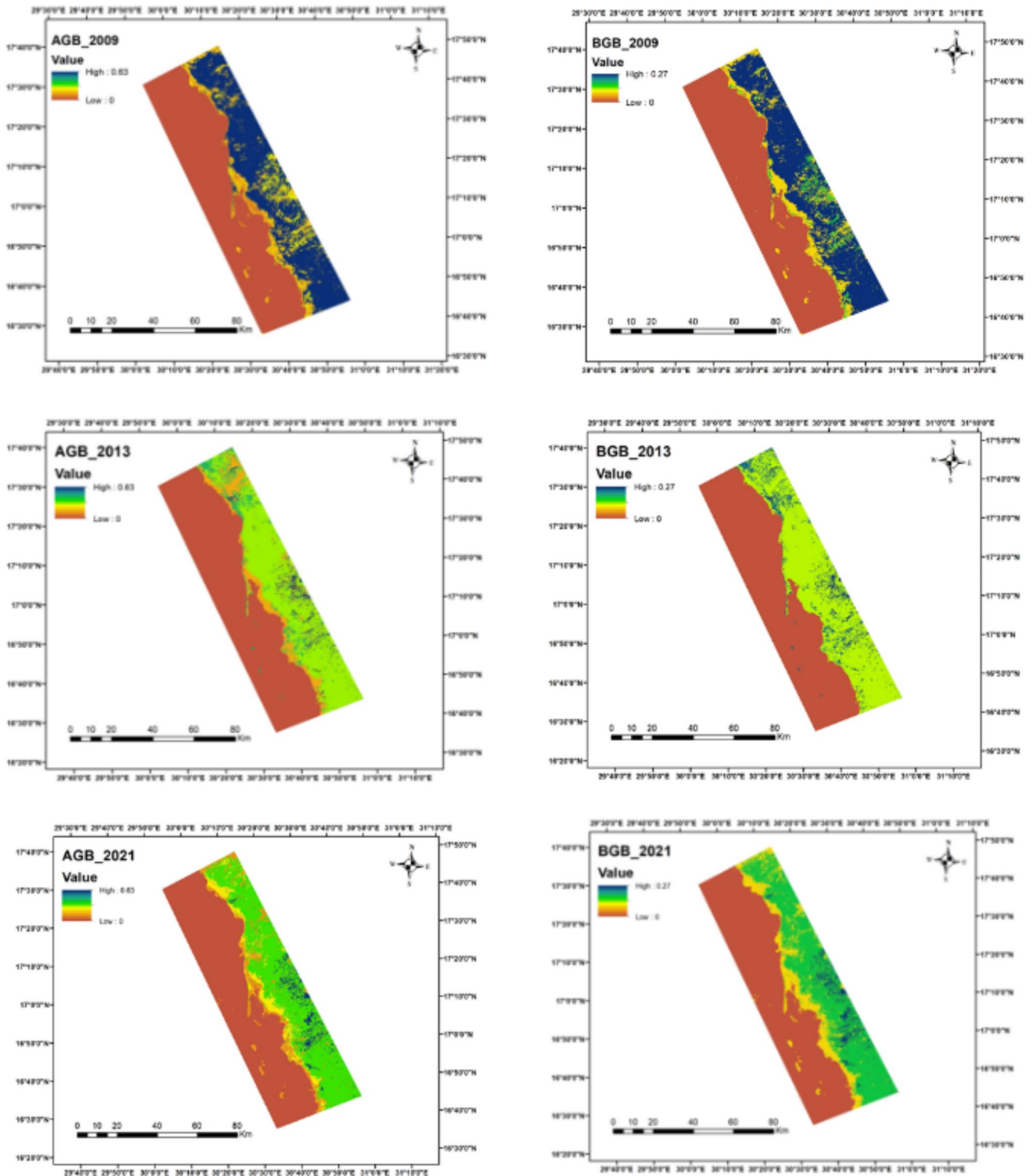


Fig. 10 Maps of value and distribution of aboveground biomass (AGB) and belowground biomass (BGB) in the study area periods

Table 6 Transition cost (\$US/km²) of carbon stock during three periods

LULC transitions	1%		3%		7%	
	Value (million \$US)	Rate (\$US/km ²)	Value (million \$US)	Rate (\$US/km ²)	Value (million \$US)	Rate (\$US/km ²)
2009_2013	-270.16	-84.47	-210.12	-82.76	-210.12	-79.35
2013_2021	269.00	84.11	209.22	82.41	209.22	79.01
2021_2031	22842.54	7142.21	17766.42	6997.92	17766.42	6709.35

Acknowledgements The authors gratefully acknowledge the contributions of Dr. Amr Keshta who kindly corrected and improved the English of the manuscript.

Authors' Contributions "All authors contributed to the study conception and design. Material preparation, data collection and analysis were performed by [Hazem T. Abd El-Hamid], [Ebrahim M. Eid] [Mohamed H.E. El-Morsy], [Hanan E.M. Osman] and [Amr E. Keshta]. The first draft of the manuscript was written by [Hazem T. Abd El-Hamid] and all authors commented on previous versions of the manuscript. All authors read and approved the final manuscript".

Funding Open access funding provided by The Science, Technology & Innovation Funding Authority (STDF) in cooperation with The Egyptian Knowledge Bank (EKB).

Data Availability All data generated or analyzed during this study are included in this published article and its supplementary information files.

Code Availability Not applicable.

Declarations

Declaration of competing interest All authors declare no conflicts of interest.

Open Access This article is licensed under a Creative Commons Attribution 4.0 International License, which permits use, sharing, adaptation, distribution and reproduction in any medium or format, as long as you give appropriate credit to the original author(s) and the source, provide a link to the Creative Commons licence, and indicate if changes were made. The images or other third party material in this article are included in the article's Creative Commons licence, unless indicated otherwise in a credit line to the material. If material is not included in the article's Creative Commons licence and your intended use is not permitted by statutory regulation or exceeds the permitted use, you will need to obtain permission directly from the copyright holder. To view a copy of this licence, visit <http://creativecommons.org/licenses/by/4.0/>.

References

- Aalde H, Gonzalez P, Gytarsky M, Krug T, Kurz WA, Lasco RD, Martino DL, McConkey BG, Ogle S, Paustian K (2006) Generic methodologies applicable to multiple land-use categories, in: Eggleston HS, Buendia L, Miwa K, Ngara T, Tanabe K (eds), IPCC Guidelines for National Greenhouse Gas Inventories. IGES, Japan
- Abbas Z, Yang G, Zhong Y, Zhao Y (2021) Spatiotemporal change analysis and future scenario of LULC using the CA-ANN approach: A case study of the Greater Bay Area. *China Land* 10:584
- Abd El-Hamid HT (2020) Geospatial analyses for assessing the driving forces of land use/land cover dynamics around the Nile Delta branches. *Egypt J Indian Soc Remote Sens* 48:1661–1674
- Abd El-Hamid HT, Caiyong W, Yongting Z (2019) Geospatial analysis of land use driving force in coal mining area: Case study in Ningdong, China. *Geo J* 86:605–620
- Abd El-Hamid HT, Hafiz MA (2022) Modeling of carbon sequestration with land use and land cover in the northeastern part of the Nile Delta, Egypt. *Arab J Geosci* 15:1267. <https://doi.org/10.1007/s12517-022-10462-2>
- Al-Hatim HY, Alrajhi D, Al-Rajab AJ (2015) Detection of pesticide residue in dams and well water in Jazan area, Saudi Arabia. *Am J Environ Sci* 11:358–365
- Arshad M, Alrumman S, Eid EM (2018) Evaluation of carbon sequestration in the sediment of polluted and non-polluted locations of mangroves. *Fund Appl Limnol* 192:53–64
- Bai J, Zhang G, Zhao Q, Lu Q, Jia J, Cui B, Liu X (2016) Depth-distribution patterns and control of soil organic carbon in coastal salt marshes with different plant covers. *Sci Rep* 6:34835
- Barbier EB, Hacker SD, Kennedy C, Koch EW, Stier AC, Silliman BR (2011) The value of estuarine and coastal ecosystem services. *Ecol Monogr* 81:169–193
- Costanza R, Ralph A, Rudolf DG, Stephen F, Grasso M, Hannon B, Limburg K, Naeem S, O'Neill RV, Paruelo J, Raskin RG, Sutton P, van den Belt M (1997) The value of the world's ecosystem services and natural capital. *Nature* 387:253–260
- Eid EM, Arshad M, Shaltout KH, El-Sheikh MA, Alfarhan AH, Picó Y, Barcelo D (2019) Effect of the conversion of mangroves into shrimp farms on carbon stock in the sediment along the southern Red Sea coast, Saudi Arabia. *Environ Res* 176:108536
- Eid EM, El-Bebany AF, Alrumman SA (2016) Distribution of soil organic carbon in the mangrove forests along the southern Saudi Arabian Red Sea coast. *Rend Fis Acc Lincei* 27:629–637
- Eid EM, Khedher KM, Ayed H, Arshad M, Moatamed A, Mouldi A (2020) Evaluation of carbon stock in the sediment of two mangrove species, *Avicennia marina* and *Rhizophora mucronata*, growing in the Farasan Islands, Saudi Arabia. *Oceanologia* 62:200–213
- Eswaran E, Van Den Berg E, Reich P (1993) Organic carbon in soils of the world. *Soil Sci Soc Am J* 57:192–194
- He C, Zhang D, Huang Q, Zhao Y (2016) Assessing the potential impacts of urban expansion on regional carbon storage by linking the LUSD-urban and InVEST models. *Environ Model Software* 75:44–58
- Howard J, Sutton-Grier A, Herr D, Kleypas J, Landis E, Mcleod E et al (2017) Clarifying the role of coastal and marine systems in climate mitigation. *Front Ecol Environ* 15:42–50
- IPCC (Intergovernmental Panel on Climate Change) (2007) In: Pachauri RK, Reisinger A (eds) *Climate Change 2007: Synthesis Report. Contribution of Working Groups I, II and III to the Fourth Assessment Report of the Intergovernmental Panel on Climate Change* [Core Writing Team. IPCC, Geneva, Switzerland, p 104
- Japelaghi M, Hajian F, Gholamalifard M, Pradhan B, Maulud KNA, Park HJ (2022) Modelling the impact of land cover changes on carbon storage and sequestration in the Central Zagros Region. *Iran Using Ecosyst Serv Approach Land* 11:423. <https://doi.org/10.3390/land11030423>

- Jiang W, Deng Y, Tang Z, Lei X, Chen Z (2017) Modelling the potential impacts of urban ecosystem changes on carbon storage under different scenarios by linking the CLUE-S and the InVEST models. *Ecol Mod* 345:30–40
- Kacem HA, Bouroubi Y, Khomalli Y, Elyaagoubi S, Maanan M, Rhinane H, Maanan M (2022) The economic benefit of coastal blue carbon stocks in a Moroccan lagoon ecosystem: A case study at Moulay Bouselham Lagoon. *Wetlands* 42:17
- Keshta AE, Riter JCA, Shaltout KH, Baldwin AH, Kearney M, Sharaf El-Din A, Eid EM (2022) Loss of coastal wetlands in Lake Burullus, Egypt: A GIS and remote-sensing study. *Sustainability* 14:4980
- Landis RJ, Koch GG (1977) The measurement of observer agreement for categorical data. *Biometrics* 33:159–174
- Lau WWY (2013) Beyond carbon: Conceptualizing payments for ecosystem services in blue forests on carbon and other marine and coastal ecosystem services. *Ocean Coast Manag* 83:5–14
- McLeod E, Chmura GL, Bouillon S, Salm R, Björk M, Duarte CM, Lovelock CE, Schlesinger WH, Silliman BR (2011) A blueprint for blue carbon: Toward an improved understanding of the role of vegetated coastal habitats in sequestering CO₂. *Front. Ecol Environ* 9:552–560
- Mekuria W (2013) Changes in regulating ecosystem services following establishing exclosures on communal grazing lands in Ethiopia: A synthesis. *J. Ecosys.* 2013, 860736
- Mishra VN, Rai PK, Mohan K (2014) Prediction of land use changes based on land change modeler (LCM) using remote sensing: A case study of Muzaffarpur (Bihar), India. *J Geogr Inst Jovan Cvijic SASA* 64:111–127
- Mulders MA (2001) Advances in the application of remote sensing and GIS for surveying mountainous land. *Int J Appl Earth Obs Geoinf* 3(1):3–10
- Ouyang X, Lee S (2013) Carbon accumulation rates in salt marsh sediments suggest high carbon storage capacity. *Biogeosci Discuss* 10:19155–19188
- Padilla FM, Vidal B, Sánchez J, Pugnaire FI (2010) Land-use changes and carbon sequestration through the twentieth century in a Mediterranean mountain ecosystem: Implications for land management. *J Environ Manage* 91:2688–2695
- Page ML (2019) Carbon dioxide levels will soar past the 410 ppm milestone in 2019. *New Sci. Mag.* 3214
- Post WM, Emmanuel WR, Zinke PJ, Stangenberger AG (1982) Soil carbon pools and world life zones. *Nature* 298:156–159
- Richards JA (2013) *Remote Sensing Digital Image Analysis: An Introduction*, vol 3. Springer, Berlin/Heidelberg, Germany
- Rumpel C, Amiraslani F, Koutika LS, Smith P, Whitehead D, Wollenberg E (2018) Put more carbon in soils to meet Paris climate pledges. *Nature* 564(7734):32–34
- Sanderman J et al (2018) A global map of mangrove forest soil carbon at 30 m spatial resolution. *Environ Res Lett* 13:055002
- Seto KC, Kaufmann RK (2003) Modeling the drivers of urban land use change in the Pearl River Delta, China: Integrating remote sensing with socioeconomic data. *Land Econ* 79:106–121
- Shaltout KH, Ahmed MT, Alrumman SA, Ahmed DA, Eid EM (2020) Evaluation of the carbon sequestration capacity of arid mangroves along nutrient availability and salinity gradients along the Red Sea coastline of Saudi Arabia. *Oceanologia* 62:56–69
- Sharma G, Sharma LK, Sharma KC (2019) Assessment of land use change and its effect on soil carbon stock using multitemporal satellite data in semiarid region of Rajasthan, India. *Ecol Process* 8:42
- Sharp R, Chaplin-Kramer R, Wood S, Guerry A, Tallis H, Ricketts T (2018) *InVEST User's Guide Integrated Valuation of Ecosystem Services and Tradeoffs Version 3.5.0*. The Natural Capital Project. Stanford University, University of Minnesota, The Nature Conservancy, and World Wildlife Fund
- Sharp R, Tallis HT, Ricketts T, Guerry AD, Wood SA, Chaplin-Kramer R, Vigerstol K (2020) *InVEST User's Guide*. The Natural Capital Project. Stanford University, University of Minnesota, The Nature Conservancy, and World Wildlife Fund
- Siikamäki J, Sanchirico JN, Jardine S, McLaughlin D, Morris DF (2012b) *Blue Carbon: Global Options for Reducing Emissions From the Degradation and Development of Coastal Ecosystems*. Resources for the Future, Washington, DC 20036
- Siikamäki J, Sanchirico J, Jardine S (2012a) Global economic potential for reducing carbon dioxide emissions from mangrove loss. *PANAS* 109:14369–14374
- Sil A, Fonseca F, Gonçalves J, Honrado J, Marta-Pedroso C, Alonso J, Ramos M, Azevedo JC (2017) Analysing carbon sequestration and storage dynamics in a changing mountain landscape in Portugal: Insights for management and planning. *Int J Biodivers Sci Ecosyst Serv Manag* 13:82–104
- Taillardat P, Friess DA, Lupascu M (2018) Mangrove blue carbon strategies for climate change mitigation are most effective at the national scale. *Biol Lett* 14:20180251
- Tallis HT, Ricketts T, Guerry AD, Wood SA, Sharp R, Nelson E, Pennington D (2013) *InVEST 2.5.6 User's Guide*. The Natural Capital Project. Stanford University, University of Minnesota, The Nature Conservancy, and World Wildlife Fund
- Villela D, de Mattos E, Pinto A, Vieira S, Martinelli L (2012) Carbon and nitrogen stock and fluxes in coastal Atlantic Forest of south-east Brazil: Potential impacts of climate change on biogeochemical functioning. *Braz J Biol* 72:633–642
- Von Neumann J (1951) The general and logical theory of automata, in: Jeffress, L.A. (Ed.), *Cerebral Mechanisms in Behavior: The Hixon Symposium*. John Wiley & Sons, New York, 1–41
- Zaitunah I A, Samsuri Ahmad AG, Safitri RA (2018) Normalized difference vegetation index (ndvi) analysis for land cover types using landsat 8 oli in besitang watershed, Indonesia. *IOP Conf Ser : Earth Environ Sci* 126:012112
- Zhao L, Peng ZR (2012) An agent-based cellular automata model of land use change developed for transportation analysis. *J Trans Geo* 25:35–49

Publisher's Note Springer Nature remains neutral with regard to jurisdictional claims in published maps and institutional affiliations.